

DOI: 10.1002/cmdc.200500061

Poly(ADP-Ribose)-Polymerase-Catalyzed Hydrolysis of NAD^+ : QM/MM Simulation of the Enzyme Reaction

Daniele Bellocchi,^[a] Gabriele Costantino,^[a] Roberto Pellicciari,^{*[a]}
 Nazzareno Re,^{*[b]} Alessandro Marrone,^[b] and Cecilia Coletti^[b]

Poly(ADP-ribose) polymerase (PARP) is a nuclear enzyme which uses NAD^+ as substrate and catalyzes the transfer of multiple units of ADP-ribose to target proteins. PARP is an attractive target for the discovery of novel therapeutic agents and PARP inhibitors are currently evaluated for the treatment of a variety of pathological conditions such as brain ischemia, inflammation, and cancer. Herein, we use the PARP-catalyzed reaction of NAD^+ hydrolysis as a model for gaining insight into the molecular de-

tails of the catalytic mechanism of PARP. The reaction has been studied in both the gas-phase and in the enzyme environment through a QM/MM approach. Our results indicate that the cleavage reaction of the nicotinamide-ribosyl bond proceeds through an $\text{S}_{\text{N}}2$ dissociative mechanism via an oxacarbenium transition structure. These results confirm the importance of the structural water molecule in the active site and may constitute the basis for the design of transition-state-based PARP inhibitors.

Introduction

Poly(ADP-ribosylation) is a transient post-translational protein modification which takes place in eukaryotes in response to DNA single-strand breaks, as well as in the epigenetic control of gene transcription through protein remodeling.^[1] The molecular effector of poly(ADP-ribosylation) is a family of nuclear enzymes, the founding member of which is poly(ADP-ribose) polymerase-1 (PARP-1), which uses NAD^+ as substrate to transfer multiple units (up to 200) of ADP-ribose to acceptor proteins, including histones, topoisomerases, and PARP-1 itself. PARP-1 is involved in a variety of processes related to the maintenance of genomic integrity, cell differentiation, and survival. Accordingly, PARP-1 is considered an attractive target for the development of therapeutic agents potentially useful in the treatment of pathological conditions such as brain^[2] and heart^[3] ischemia, inflammation,^[4] and cancer.^[5]

Kinetic analysis,^[6] mutational studies,^[7,8] and crystallographic determinations^[9–12] have permitted quite a clear elucidation of the catalytic potentiality of PARP-1. In particular, PARP-1 is endowed with the following activities (Scheme 1): 1) PARP-1 binds NAD^+ and promotes the initiation of poly(ADP-ribose) (PAR) polymer formation by transferring the first unit of ADP-ribose to the acceptor protein; 2) PARP-1 catalyzes the elongation reaction, in which multiple ADP-ribose units are subsequently attached to the nascent PAR–protein conjugate through the formation of 1,2 α -glycosidic bonds; and 3) PARP-1 is also endowed with an NAD^+ -hydrolytic activity.^[7] The biological significance of this latter activity is not clear, but it should be related to the ability of the enzyme to compete between the initiation of a new PAR chain or the hydrolysis of NAD^+ .

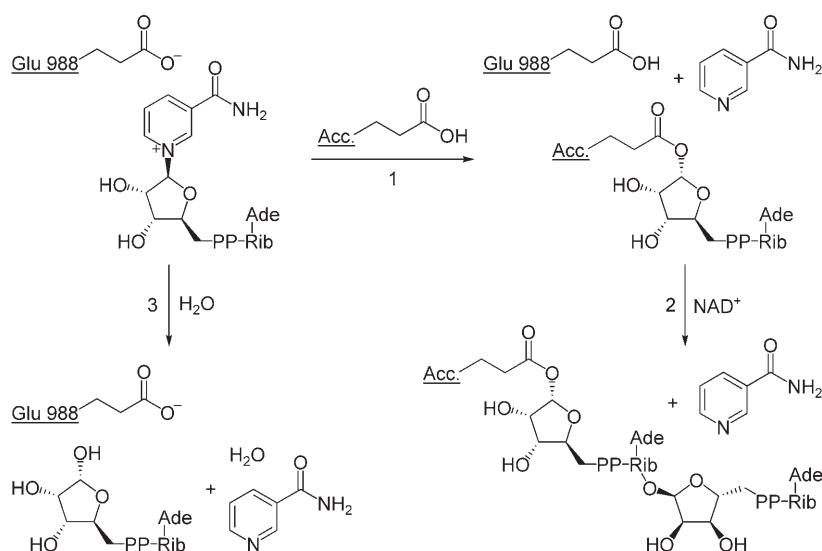
Common to all these processes and reminiscent of the mechanism employed by prokaryotic mono(ADP-ribose) trans-

ferases such as diphtheria, cholera, and pertussis toxins is the enzyme-catalyzed nucleophilic attack by a glutamic acid residue of an acceptor protein (case 1), or by a water molecule (case 3) on the ribose C1-anomeric carbon atom (Scheme 1). An important role is played by a highly conserved residue, namely Glu988 (based on the residue numbering for hPARP-1, conserved as Glu148 in diphtheria toxin and as Glu129 in pertussis toxin), which is thought to promote the nucleophilic attack on the C1-anomeric carbon atom by acting as a general-base catalyst.^[7,8,13,14]

The ability to fully elucidate the molecular details of the reaction can be central to the design of novel mechanism-based PARP-1 inhibitors. In this context, the NAD^+ hydrolysis reaction (path 3, Scheme 1), in which a water molecule acts as a nucleophile to attack the C1-anomeric carbon atom of the ribose moiety, is of particular interest. First, this reaction can be taken as a model for the general nucleophilic attack reaction; second, the catalytically relevant water molecule may also play a role in determining the binding orientation of competitive PARP-1 inhibitors.^[15]

[a] Dr. D. Bellocchi, Prof. G. Costantino, Prof. R. Pellicciari
 Dipartimento di Chimica e Tecnologia del Farmaco
 Università degli Studi di Perugia
 Via del Liceo 1, 06123 Perugia (Italy)
 Fax: (+39) 075-585-5124
 E-mail: rp@unipg.it

[b] Prof. N. Re, Dr. A. Marrone, Dr. C. Coletti
 Facoltà di Farmacia
 Università G. D'Annunzio
 Via dei Vestini 13, 66100, Chieti (Italy)
 Fax: (+39) 0871-355-5267
 E-mail: nre@unich.it



Scheme 1. PARP-1 activities.

Understanding the details of bond-breaking and bond-forming steps as well as the structure of the transition state(s) requires the use of quantum mechanics (QM) approaches. These approaches are usually limited by their computational load. To make QM studies of chemical reactions in large systems computationally more feasible, combined quantum mechanical/molecular mechanical (QM/MM) methods have been developed. The idea, introduced first by Levitt and Warshel in 1976,^[16] is to divide the system into a part which is treated accurately by means of QM, whereas the rest is approximated using MM methods.

Herein, we report a QM/MM study aimed at the description of the reaction coordinate for NAD⁺ hydrolysis, the identification of the transition state for this reaction, and unraveling the enzyme's effect in transition-state stabilization.

Methods

Model building

A QM/MM model of the PARP–NAD⁺–H₂O system was built on the basis of the crystal structures of the ternary complex diphtheria toxin (DT)–NAD⁺–H₂O (1tox)^[17] and of the binary complex PARP–3-methoxybenzamide (3MBA) (3pax),^[10] retrieved from the RCSB Protein Data Bank. A starting geometry was first built from the PARP–NAD⁺–H₂O ternary complex in which the location of water and NAD⁺ reflects the experimentally detected configuration of the DT complex, and is thus a reasonable approximation of the real ternary Michaelis adduct that initiates the PARP-catalyzed hydrolysis of NAD⁺. This result was triggered according to the scheme suggested by Ruf et al.^[10] The approach relies on the exploitation of the DT–co-substrates crystallographic geometry as a template for the binding configuration of the PARP ternary complex. In more detail, the catalytic domains of the DT and PARP complexes were superimposed, minimizing the rms deviation. The NAD⁺ molecule

was then rigidly located by superimposing its nicotinamide moiety onto the highly homologous 3MBA. An enzyme–ligand structure of PARP was obtained in which: 1) a water molecule, derived from the 1tox structure, lies close to the ribose group of NAD⁺ and 2) the position of the nicotinamide moiety of NAD⁺ resembles that of the co-crystallized PARP inhibitor 3MBA. We focused on the hydrolysis reaction, involving C1 of the nicotinamide-binding ribose and replaced the ADP moiety bound to it in the NAD⁺ group with a hydrogen atom. This subsystem is shown in Figure 1 and will be hereafter called NR. The PARP–NR–H₂O complex was relaxed

using the Charmm27 force field implemented in the Insight II program,^[18] and the resulting geometry was used as the reference structure for subsequent calculations.

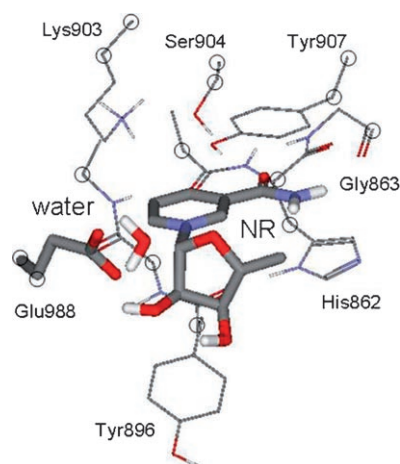


Figure 1. QM/MM partition scheme: the QM portion (Glu 988, NR, water) is in stick representation, whereas lines represent the remaining MM portion (PARP active site, side chain, and backbone residues). Frozen coordinates are highlighted by circles.

Gas-phase calculations

AM1 calculations were performed for the study of NR hydrolysis in the gas phase. Semiempirical methods such as AM1 often overestimate barriers,^[19] and therefore, higher-level calculations (B3LYP/6-31 + G(d)) on AM1-optimized geometries were performed to correct the reaction energies. Similar approaches have been successfully employed in modeling other enzymes.^[20,21]

The starting geometry of the reactants (R), that is, water approaching C1 of the NR, was taken, as described above, from the PARP–co-substrates complex. Assuming an S_N2 A_ND_N mech-

anism of hydrolysis,^[22,23] the geometry of R was modified to generate starting structures for the geometry optimization of the transition state (TS) and products (P). The former was built by decreasing the distance between the nucleophile (water) and C1 and increasing the distance between the leaving group (nicotinamide) and C1, and by flattening the ribose substrate such that the sp^2 character of C1, C2, and O4 is maximal at the TS (see below). Next, the P input structure was obtained from the input of the TS by increasing the distance of the nicotinamide molecule from C1.

The geometry optimization of both R and P was performed without constraints by using the Berny algorithm, whereas the TS geometry was optimized by using the eigenvector-following method.^[24,25] The topology of all the calculated stationary points of the potential energy surface (PES)—R and P minima and TS—was checked through vibrational frequency calculations at the same level of theory. Intrinsic reaction coordinate (IRC) calculations were further carried out to confirm that the calculated stationary points were connected in the PES. Finally, single-point energy calculations were performed at the B3LYP/6-31G+(d) level for the characterization of the PES. All calculations were carried out by using the Gaussian program package.^[26] Electrostatic potentials mapped onto isodensity surfaces of the stationary points were obtained by carrying out AM1 calculations using the ArgusLab 3.1 software package.^[27]

QM/MM calculations

The main problem of QM/MM approaches lies in the correct treatment of the boundary between QM and MM regions. Indeed, the separation of covalently bonded atoms in these regions introduces unsaturated valences in the QM part. A number of approaches have been proposed to circumvent this problem, such as the frozen-orbital,^[16] or the link-atoms approach.^[28] The latter is used in the ONIOM scheme,^[29,30] which was employed in the present investigation.

The NR hydrolysis reaction was investigated within the PARP catalytic domain. Owing to the complexity of the model system, that is, the PARP-co-substrates complex described above, only the side chains of the residues and backbone atoms lying within 8 Å of the NR (Figure 1) were explicitly considered. These protein fragments directly interact with the hydrolysis reaction core—the subsystem formed by water and NR—and are thus crucial to correctly describe the enzyme catalytic effect (see below). QM/MM calculations were carried out by applying the two-layered ONIOM2 scheme to the reduced model system, as implemented in the Gaussian98 program package.^[31] The QM region was treated at the AM1 semiempirical level of theory, whereas the Dreiding all-atom force fields were applied to the MM region. The ONIOM partition scheme we assumed in this study is sketched in Figure 1. The QM region includes NR, the water molecule, and the Glu988 side chain, which has been indicated as essential for enzyme catalysis.^[7,8] As shown in Figure 1, the QM edge is mainly non-covalent, and the $C^\alpha-C^\beta$ bond of the Glu988 residue is the only covalent bond breaking within such a partition scheme. The C^α atom of Glu988 was replaced by a hydrogen atom in the QM

part of the ONIOM calculation (the default in ONIOM). As the MM region consists of fragments cut from the whole PARP catalytic domain, it was constrained to keep the “enzyme-like location” of the side chains of the involved residues and to avoid possible steric inconsistencies during the optimization runs, such as an unrealistic blow-up of the model system. This has been done by freezing the atomic coordinates indicated by circles in Figure 1. The geometry of R, P and TS was calculated for the NR hydrolysis at AM1/Dreiding level of theory within such a partition and constraint pattern. The NR-water geometries of the R, TS, and P calculated at the AM1 level of theory in the gas phase were employed to create the corresponding input structures for ONIOM optimizations. As IRC calculations cannot be performed by using the AM1/Dreiding ONIOM scheme, an approximated approach was set up to check the connection in the PES between R, TS, and P. In particular, the TS geometry was perturbed along the reaction-associated eigenvector obtained by frequency calculations. The TS geometry was accordingly modified to obtain the input geometry of both product-like and reactant-like structures. The resulting geometries were then optimized through a sequence of five Steepest Descent (SD) minimization runs, each one consisting of ten SD steps with explicit calculation of the energy derivatives, followed by a Berny optimization. All the calculated stationary points were checked through vibrational frequency calculations at the AM1 level of theory. To compare ONIOM results with those of the gas phase, single-point calculations were performed at the B3LYP/6-31+G(d) level of theory on the reduced model system.

Results

Gas-phase calculations

Figure 2 shows the energy outline (B3LYP/6-31+G(d)) of the NR hydrolysis in the gas phase, and Figure 3 illustrates the optimized geometries and the electrostatic potential mapped

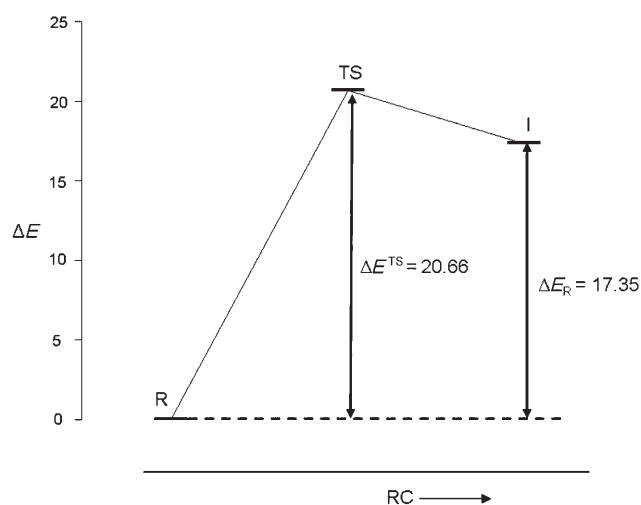


Figure 2. Reaction profile for NAD^+ hydrolysis in the gas phase; ΔE : relative energy (kcal mol^{-1}), RC: reaction coordinate.

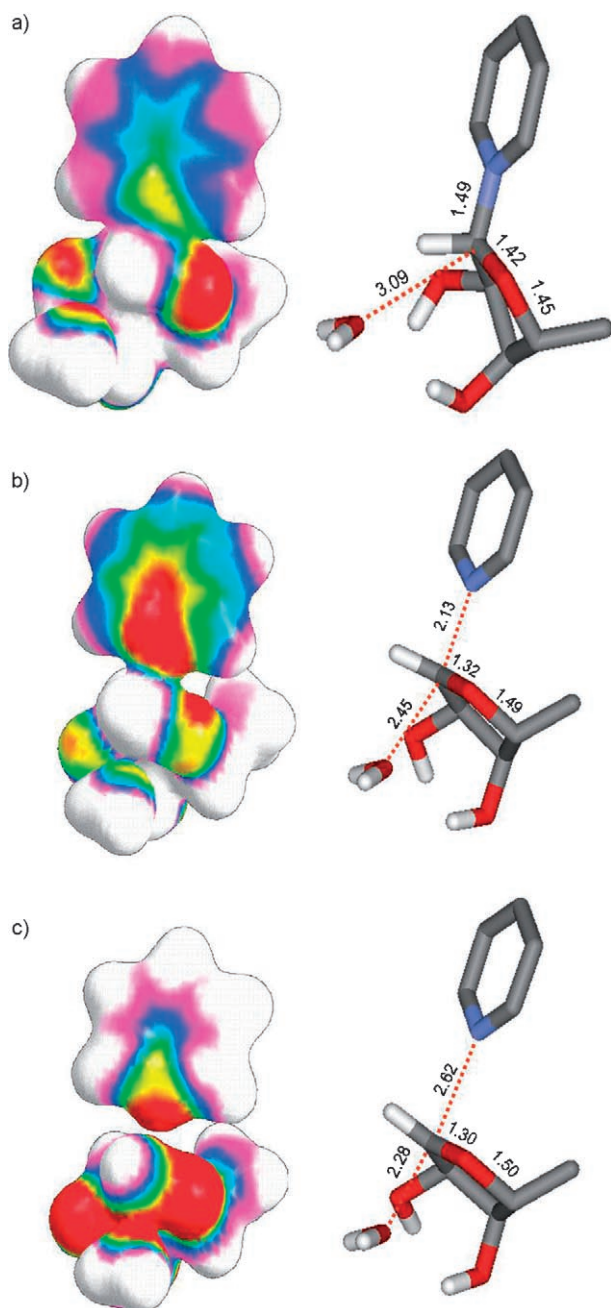


Figure 3. Gas-phase calculations: AM1-optimized geometries and electrostatic-potential-mapped isosurfaces (contour value: 0.05, map values: ± 0.05) for a) R, b) TS, and c) P.

onto isosurfaces of the NR-water reactant, transition state, and product systems.

Frequency calculations on the TS structure provide only one imaginary value (-247 cm^{-1}) associated with a stretching movement along the reaction coordinate that corresponds to bond disruption and formation; the result is illustrated by dotted red lines in Figure 3, and is consistent with the expected $S_N2 A_N D_N$ mechanism.^[22,23] Frequency analysis of the product I does not show any negative eigenvalue, thus confirming that this species is a stable oxacarbenium ion,^[32] even if its energy is very close to that of the TS. The overall energy profile

of Figure 2 shows an activation energy of $20.66\text{ kcal mol}^{-1}$ for the NAD^+ hydrolysis reaction, for which an activation enthalpy of $25.2\text{ kcal mol}^{-1}$ has been estimated.^[33]

QM/MM calculations

Figure 4 shows the ONIOM2^[31] (AM1/Dreiding)-optimized geometries of the NR-water reactant (Michaelis complex), transition state, and final product of the hydrolysis reaction at the PARP active site. In Figure 5, the energy profile along the reaction coordinate of the PARP-catalyzed NR hydrolysis (B3LYP/6-31+G(d) single-point calculations on geometry optimized at the QM/MM level) is displayed and shows an activation energy of $7.26\text{ kcal mol}^{-1}$. Due to the presence of geometry constraints (Figure 1), frequency calculations for TS characterization produce more than one negative frequency. The largest among these (-279 cm^{-1}) is associated with a stretching movement along the reaction coordinate, corresponding to the formation and breaking of the bonds, and is displayed in red in Figure 4. All the other negative frequencies are associated with frozen atoms. The geometries of R and P (Figure 6) were obtained starting from TS geometry following the eigenvector direction associated with the reaction coordinate according to the computational scheme described above.

Discussion

Gas-phase calculations

It is widely agreed that nucleophilic substitution reactions of glycosides and related compounds proceed through transition states with substantial oxacarbenium ion character in the glycone. These reactions are on the borderline between $D_N + A_N$ (S_N1) and $A_N D_N$ (S_N2) mechanisms (Scheme 2).^[32-34] A previous semiempirical study of the gas-phase TS of nicotinamide riboside hydrolysis indicated a highly oxacarbenium-ion-like TS structure, which suggests the ability of semiempirical approaches to correctly describe this type of reactive system.^[35] In this study, the gas-phase reaction is described by an oxacarbenium-ion-like TS structure with bond distances of C1-N (leaving group) and C1-O (incoming water group) of 2.13 and 2.45 Å, respectively (Figure 3 b). According to IUPAC nomenclature, this is a concerted $S_N2 A_N D_N$ reaction in which there is a low bond order between the reactive center (ribose anomeric carbon atom, C1) and the entering and leaving groups in the transition-state structure.^[36-38]

Figure 3 shows that the breaking of the C1-anomeric carbon-pyridine nitrogen bond in the $R \rightarrow TS$ step is accompanied by a partial transfer of positive charge from the nitrogen atom to C1. Simultaneously, the latter carbon atom acquires an sp^2 hybridization, which is stabilized through the interaction of the empty p orbital with the lone pair of the oxygen atom of the incoming water molecule and that of N1. This picture is confirmed by analyzing the variation of bond lengths and charge transfer characterizing the shift between reactant and transition state. The $R \rightarrow TS$ evolution also leads to a substantial flattening of the ribose ring. Indeed, with the

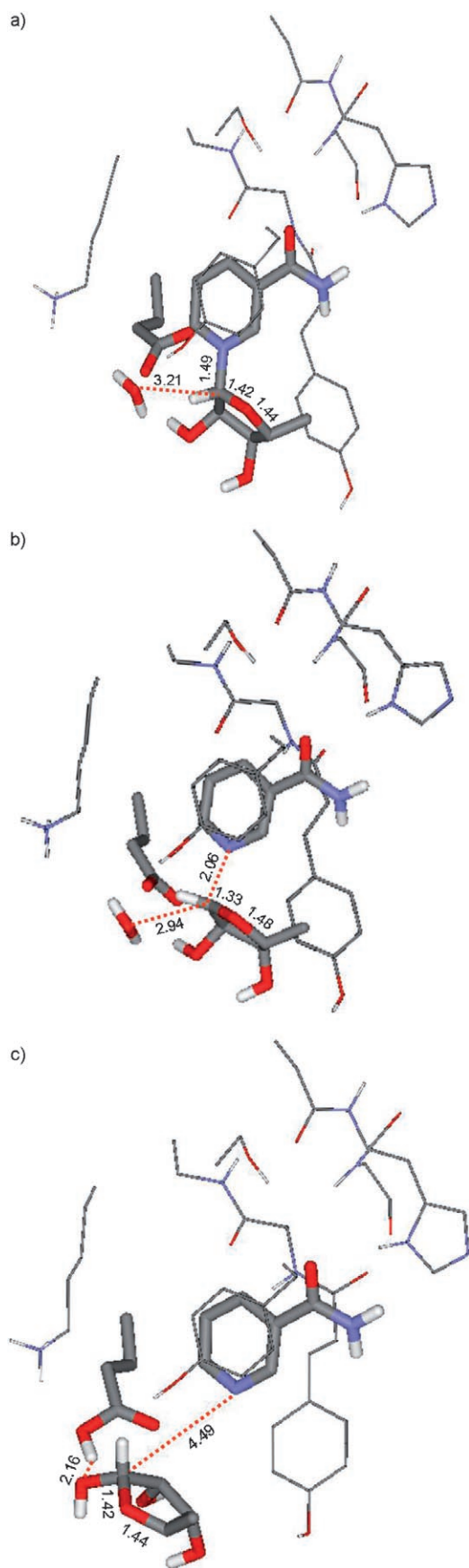


Figure 4. QM/MM calculations: ONIOM2 (AM1/Dreiding)-optimized geometries of a) R, b) TS, and c) P.

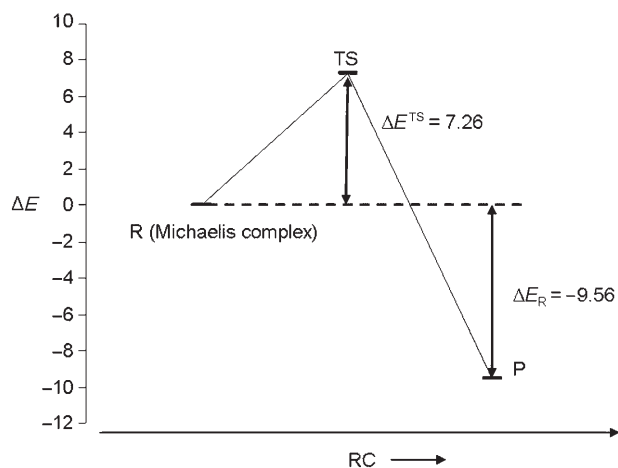


Figure 5. Reaction profile for PARP-catalyzed hydrolysis of NAD^+ ; ΔE : relative energy (kcal mol^{-1}), RC: reaction coordinate.

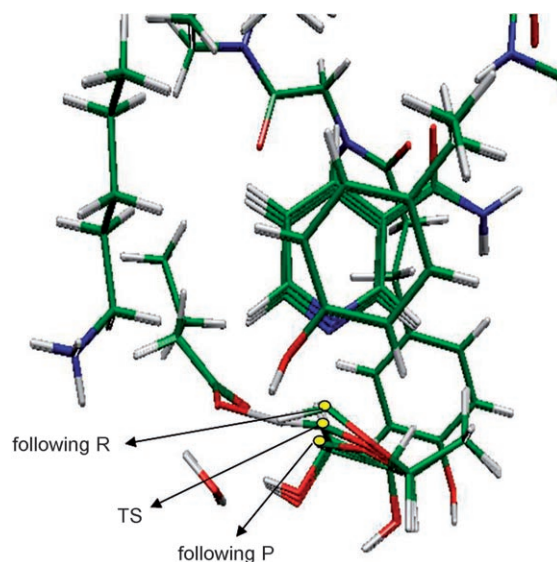
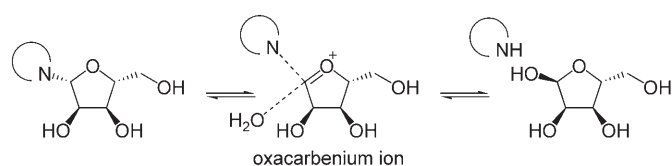


Figure 6. Eigenvector-following method: overlapping of TS geometry and input geometry of both product-like and reactant-like structures obtained by variation of the TS geometry along the reaction-associated eigenvector.



Scheme 2. Nucleophilic substitution at the C1 anomeric carbon atom of ribose.

increased sp^2 character of C1, the atoms C4, O4, C2, and C1 become coplanar, leaving out only C3 in a 3-exo fashion.

In the final evolution from transition state to product I, Figure 3c shows the completion of the positive-charge transfer from the pyridine nitrogen atom to the ribose ring. The slight stabilization of the oxocarbenium cation ($3.31 \text{ kcal mol}^{-1}$,

Figure 2) can be attributed to the enhanced interaction with the nearest lone pair of the water molecule.

QM/MM calculations

The reaction is described by a high oxocarbenium-ion-like transition structure^[32–34] with the distance for C1–N (leaving group) and C1–O (incoming water molecule) of 2.06 and 2.94 Å, respectively (Figure 4b). Going from R (Michaelis complex, Figure 4a) to TS (Figure 4b), our calculations show the same trend observed for gas phase, suggesting the partial formation of a double bond between C1 and O4 (π -electron delocalization due to the resulting sp^2 hybridization) and an S_N2 A_ND_N dissociative mechanism.^[36–38] These results are in agreement with previous studies in which the TS was characterized through kinetic isotopic effect (KIE) based on other members of the ART (ADP-ribosyltransferase) family, which share a high level of structural homology with the active site residues of PARP. Indeed, even for NAD^+ hydrolysis catalyzed by diphtheria,^[23] cholera^[39] and pertussis^[40] toxins, an oxocarbenium-ion-like TS can be observed. However, the profile of the enzymatic reaction shows relevant differences compared with the gas-phase profile discussed above. These differences are due to the presence of active-site residues whose contribution to the catalytic process is described below.

The role of Glu988 emerging from these calculations is notable. As already highlighted by mutagenesis experiments,^[7,8] the E988Q, E988A, and E988D mutations decrease the poly-(ADP-ribose) elongation, whereas E988K exclusively catalyzes mono(ADP-ribosylation).^[8] These results are similar to mutagenesis studies performed on mono(ADP-ribose) transferase toxins in which the substitution of Glu148 in the diphtheria toxin^[13] and Glu129 in the pertussis toxin^[14] led to a remarkable decrease in ADP-ribosylation activity. This is not surprising if one takes into account that PARP and ADP-ribosylating toxins belong to the same ART family and catalyze the same reactions, namely ADP-ribosylation and NAD^+ hydrolysis (Scheme 1). In these reactions, a glutamate residue, which is invariably conserved and localized in a strategic region of the active site, is considered to play a key role as a general base by activating nucleophilic attack in which water is the nucleophile in hydrolysis and an amino acid acceptor is the nucleophile in the ADP-ribosyltransferase reaction, Scheme 1. The present study confirms the importance of this residue in the catalytic process. In particular, 1) it stabilizes the Michaelis complex, favoring the positioning of a water molecule very close to the reactive center (C1-anomeric carbon) by forming a network of hydrogen bonds with the water molecule and the 2-hydroxy group of ribose (Figure 4a) and 2) it is suitably oriented for potential electrostatic stabilization of the dipolar TS (electrostatic catalysis) (Figure 4b). This orientation is achieved by a rotation of the carboxylic group ($\sim 90^\circ$), which is necessary for adjusting hydrogen extraction and to optimize delocalization of the positive charge on the ribose ring (C1–O4–C2). These results are in agreement with a molecular dynamics study of the diphtheria-toxin-catalyzed hydrolysis of NAD^+ ,

which also indicates a direct electrostatic stabilization of the ribo-oxocarbenium-ion-like TS.^[41]

Figure 4c shows the final catalytic path in which Glu988 abstracts a hydrogen atom from the water molecule, allowing the insertion of a hydroxide group at the reactive center C1. The NAD^+ hydrolysis mechanism resembles the ADP-ribosylating mechanism, which requires the presence of a hydrogen-bond acceptor close to the water molecule. In both cases, nucleophilic attack by a hydroxide moiety (hydrolysis) or by an acceptor protein/ribose alkoxide^[6] (ADP-ribosyltransferase reaction), leads to an inversion of configuration at C1, as is the case for ADP-ribosylating toxins.^[42]

Figure 5 displays the energy profile along the reaction coordinate. The low activation energy of $7.26 \text{ kcal mol}^{-1}$ for the PARP-catalyzed NAD^+ hydrolysis reflects once more the relative stability of the oxocarbenium ion complex.^[33]

Finally, Figure 7 shows a comparison of the energy profiles for the gas-phase and PARP-catalyzed reactions and shows that the presence of the PARP active site lowers the activation

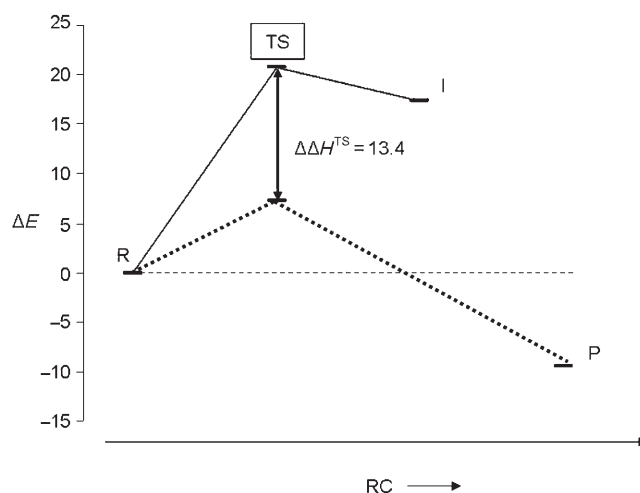


Figure 7. Comparison of the AM1 energy profile along the optimized reaction coordinate (RC) for PARP-catalyzed (.....) and gas-phase (—) NAD^+ hydrolysis.

energy by $13.4 \text{ kcal mol}^{-1}$, most of which is probably due to the inclusion of Glu988 in the QM region. This difference in the activation energy is in good agreement with the observed 6000-fold rate acceleration for diphtheria toxin-catalyzed NAD^+ hydrolysis relative to the noncatalyzed reaction.^[41]

Conclusions

The NAD^+ hydrolysis mechanism catalyzed by PARP has been investigated for the first time through a QM/MM approach. The results indicate that both the gas-phase and enzyme-catalyzed cleavage of the nicotinamide-ribose bond proceeds through an S_N2 dissociative mechanism via an oxocarbenium transition-state structure and intermediate, in agreement with the results of Oppenheimer.^[43] Taking into account the high level of similarity within the active sites of the ADP-ribosyl-

transferase (ART) family, and in particular the presence of an invariably conserved glutamate residue, it is reasonable to suppose that the results obtained for the PARP enzyme can be useful for understanding the catalytic mechanism of other ARTs of pharmacological importance, such as virulent factors of prokaryotic pathogens, in particular ADP-ribosylating toxins, and enzymes that belong to the ecto-ART family (rART2.2).^[44] These, together with the PARP family, represent the only structure of eukaryotic ARTs that have been characterized so far. Particularly interesting is the role of a water molecule in the PARP active site which has become apparent from the present study. The water molecule is not only involved in the hydrolysis mechanism of NAD⁺, but as we have already reported, is also involved in bond stability of PARP inhibitors; in fact, it should be considered part of their hydration shell.^[15] These results suggest the potential success of new PARP inhibitors with a design based on transition-state structure.

Keywords: enzymes · inhibitors · molecular modeling · poly(ADP-ribose) polymerase · reaction mechanisms

- [1] R. Pellicciari, E. Camaioni, G. Costantino, *Prog. Med. Chem.* **2004**, *44*, 125–169.
- [2] J. Zhang, V. L. Dawson, T. M. Dawson, S. H. Snyder, *Science* **1994**, *263*, 687–689.
- [3] C. Thiemermann, J. Bowes, F. P. Myint, J. R. Vane, *Proc. Natl. Acad. Sci. USA* **1997**, *94*, 679–683.
- [4] C. Sharp, A. Warren, T. Oshima, L. Williams, J. H. Li, J. S. Alexander, *Inflammation* **2001**, *25*, 157–163.
- [5] C. A. Delaney, L. Z. Wang, S. Kyle, A. W. White, A. H. Calvert, N. J. Curtin, B. W. Durkacz, Z. Hostomsky, D. R. Newell, *Clin. Cancer Res.* **2000**, *6*, 2860–2867.
- [6] M. Miwa, M. Ishihara, S. Takishima, N. Takasuka, M. Maeda, Z. Yamaizumi, T. Sugimura, S. Yokoyama, T. Miyazawa, *J. Biol. Chem.* **1981**, *256*, 2916–2921.
- [7] G. T. Marsischky, B. A. Wilson, R. J. Collier, *J. Biol. Chem.* **1995**, *270*, 3247–3254.
- [8] V. Rolli, M. O'Farrell, J. Menissier-de Murcia, G. de Murcia, *Biochemistry* **1997**, *36*, 12147–12154.
- [9] A. Ruf, J. Menissier-de Murcia, G. de Murcia, G. E. Schulz, *Proc. Natl. Acad. Sci. USA* **1996**, *93*, 7481–7485.
- [10] A. Ruf, G. de Murcia, G. E. Schulz, *Biochemistry* **1998**, *37*, 3893–3900.
- [11] A. W. White, R. Almassy, A. H. Calvert, N. J. Curtin, R. J. Griffin, Z. Hostomsky, K. Maegley, D. R. Newell, S. Srinivasan, B. T. Golding, *J. Med. Chem.* **2000**, *43*, 4084–4097.
- [12] T. Kinoshita, I. Nakanishi, M. Warizaya, A. Iwashita, Y. Kido, K. Hattori, T. Fujii, *FEBS Lett.* **2004**, *556*, 43–46.
- [13] B. A. Wilson, K. A. Reich, B. R. Weinstein, R. J. Collier, *Biochemistry* **1990**, *29*, 8643–8651.
- [14] R. Antoine, A. Tallett, S. van Heyningen, C. Loch, *J. Biol. Chem.* **1993**, *268*, 24149–24155.
- [15] D. Bellocchi, A. Macchiarulo, G. Costantino, R. Pellicciari, *Bioorg. Med. Chem.* **2005**, *13*, 1151–1157.
- [16] A. Warshel, M. Levitt, *J. Mol. Biol.* **1976**, *103*, 227–249.
- [17] C. E. Bell, D. Eisenberg, *Biochemistry* **1996**, *35*, 1137–1149.
- [18] Insight II, 3L **2000**, Molecular Modeling Software, Accelrys Inc. <http://www.accelrys.com>.
- [19] A. J. Mulholland, P. D. Lyne, M. Karplus, *J. Am. Chem. Soc.* **2000**, *122*, 534–535.
- [20] J. C. Hermann, C. Hensen, L. Ridder, A. J. Mulholland, H. D. Holtje, *J. Am. Chem. Soc.* **2005**, *127*, 4454–4465.
- [21] A. Lodola, M. Mor, J. C. Hermann, G. Tarzia, D. Piomelli, A. J. Mulholland, *Chem. Commun.* **2005**, *35*, 4399–4401.
- [22] P. J. Berti, V. L. Schramm, *J. Am. Chem. Soc.* **1997**, *119*, 12069–12078.
- [23] P. J. Berti, S. R. Blanke, V. L. Schramm, *J. Am. Chem. Soc.* **1997**, *119*, 12079–12088.
- [24] C. J. Cerian, W. H. Miller, *J. Chem. Phys.* **1981**, *75*, 2800.
- [25] J. Simons, P. Jørgensen, H. Taylor, J. Ozment, *J. Phys. Chem.* **1983**, *87*, 2745–2753.
- [26] M. J. Field, *J. Comput. Chem.* **2002**, *23*, 48–58.
- [27] M. Svensson, S. Humbel, R. D. J. Froese, T. Matsubara, S. Sieber, K. Morokuma, *J. Phys. Chem.* **1996**, *100*, 19357–19363.
- [28] S. Humbel, S. Sieber, K. Morokuma, *J. Chem. Phys.* **1996**, *105*, 1959–1967.
- [29] M. J. Frisch et al., Gaussian99 **2000**, Development version (Revision B.09+) Gaussian Inc., Pittsburgh, PA.
- [30] M. A. Thompson, ArgusLab 3.1 **2003**, Planaria Software LLC, Seattle, WA <http://www.arguslab.com>.
- [31] S. Dapprich, I. Komáromi, K. S. Byun, K. Morokuma, *J. Mol. Struct.* **1999**, *461–462*, 1–21.
- [32] N. S. Banait, W. P. Jencks, *J. Am. Chem. Soc.* **1991**, *113*, 7951–7958.
- [33] X. Huang, C. Surry, T. Hiebert, A. J. Bennet, *J. Am. Chem. Soc.* **1995**, *117*, 10614–10621.
- [34] M. L. Sinnott, *Chem. Rev.* **1990**, *90*, 1171–1202.
- [35] S. Schroeder, N. Buckley, N. J. Oppenheimer, P. A. Kollman, *J. Am. Chem. Soc.* **1992**, *114*, 8232–8238.
- [36] R. W. Johnson, T. M. Marschner, N. J. Oppenheimer, *J. Am. Chem. Soc.* **1988**, *110*, 2257–2263.
- [37] J. T. Stivers, Y. L. Jiang, *Chem. Rev.* **2003**, *103*, 2729–2760.
- [38] R. D. Guthrie, W. P. Jencks, *Acc. Chem. Res.* **1989**, *22*, 343–349.
- [39] K. A. Rising, V. L. Schramm, *J. Am. Chem. Soc.* **1997**, *119*, 27–37.
- [40] J. Scheuring, V. L. Schramm, *Biochemistry* **1997**, *36*, 4526–4534.
- [41] K. Kahn, T. C. Bruice, *J. Am. Chem. Soc.* **2001**, *123*, 11960–11969.
- [42] N. J. Oppenheimer, J. W. Bodley, *J. Biol. Chem.* **1981**, *256*, 8579–8581.
- [43] N. J. Oppenheimer, *Mol. Cell. Biochem.* **1994**, *138*, 245–251.
- [44] H. Ritter, F. Koch-Nolte, V. E. Marquez, G. E. Schulz, *Biochemistry* **2003**, *42*, 10155–10162.

Received: October 11, 2005

Published online on March 3, 2006